

# Characterization of a Botybirnavirus Conferring Hypovirulence in the Pear Stem Wart Disease Phytopathogenic Fungus *Botryosphaeria dothidea*

Lifeng Zhai<sup>1,2,†</sup>, Mengmeng Yang<sup>2,3†</sup>, Meixin Zhang<sup>1</sup>, Ni Hong<sup>2,3</sup>, and Guoping Wang<sup>2,3\*</sup>

<sup>1</sup> College of Life Science and Technology, Yangtze Normal University, Chongqing, China

<sup>2</sup> National Key Laboratory of Agromicrobiology, Huazhong Agricultural University, Wuhan, China

<sup>3</sup> College of Plant Science and Technology, Huazhong Agricultural University, Wuhan, China

† These authors contributed equally to this study.

\*Corresponding author: Guoping Wang; E-mail: gpwang@mail.hzau.edu.cn; Tel: +86-027-8728755339; Fax: +86-027-873846

## ABSTRACT

A double-stranded RNA (dsRNA) virus was isolated and characterized from a strain EW220 of the phytopathogenic fungus *Botryosphaeria dothidea*. The full-length cDNAs of dsRNAs were 6,434 bp and 5,986 bp in size, respectively. The largest dsRNA of BdBRV1 encodes a cap-pol fusion protein that contains part coat protein gene and a RNA-dependent RNA polymerase (RdRp) domain, and the second dsRNA encodes a hypothetical protein. The dsRNA virus was named *Botryosphaeria dothidea botybirnavirus 1* (BdBRV1). BdBRV1 contains spherical virions that are 37 nm in diameter consisting of two segments. The structural proteins of BdBRV1 virus particles were 110 kDa, 90 kDa, and 80 kDa, which encoded by dsRNA1 and 2-ORFs. The analysis of genome sequences revealed that the sequences of BdBRV1 shared 99% identity with *Bipolaris maydis botybirnavirus 1* (BmBRV1). Phylogenetic reconstruction indicated that BdBRV1 and BmBRV1 are phylogenetically related to the genus *Botybirnavirus*. Importantly, BdBRV1 influences the growth of *B. dothidea* and confers hypovirulence to the fungal host. BdBRV1 and BmBRV1 were two strains of the same virus. To our knowledge, this is the first report of a botybirnavirus in *B. dothidea* and our result might be the first finding in the different fungi infected by the same virus.

Keywords: *Botryosphaeria dothidea botybirnavirus 1*, Hypovirulence, *Botybirnavirus*, Genome, *Botryosphaeria dothidea*, double-stranded RNA virus

## Introduction

Mycoviruses have been reported from a wide range of fungal species [1–4]. The majority of mycoviruses reported to date consist of double-stranded RNA (dsRNA) and positive-sense single-stranded RNA (+ssRNA), whereas the rest possess negative-sense single-stranded RNA (-ssRNA) and single-stranded DNA (ssDNA) as their genetic material [1, 4–10]. DsRNA mycoviruses are classified into seven families, namely, *Totiviridae*, *Chrysoviridae*, *Megabirnaviridae*, *Partitiviridae*, *Quadriviridae*, *Reoviridae*, and *Endornaviridae* [1, 4]. A proposed dsRNA virus family *Botybirnaviridae* has been presented, which includes the newly reported bipartite dsRNA virus *Botrytis porri* botybirnavirus 1 (BpRV1) [11]. The family *Botybirnaviridae* presently includes six members, including BpRV1, *Sclerotinia sclerotiorum* botybirnavirus 1 (SsBRV1), SsBRV2, *Alternaria botybirnavirus* 1 (ABRV1), *Bipolaris maydis* botybirnavirus 1 (BmBRV1), and *Soybean leaf-associated botybirnavirus* 1 (SlaBRV1) [11–16]. In general, mycoviruses cause mild or no obvious effects on their hosts [1], but some can increase mycelial growth [17], reduce virulence and suppress growth of their hosts [3, 4, 11, 18–25]. The hypovirulence-associated mycoviruses have an exploitable potential for controlling diseases and thus may be utilized as biocontrol agents [3, 4, 18].

*Botryosphaeria dothidea* is capable of infecting a broad range of hosts [26, 27]. The pathogen causes stem warts, stem cankers, and fruit rot diseases in apple, pear, and grape trees in China [28–31]. Mycoviruses infecting *B. dothidea* have recently been isolated and characterized [21, 24, 32, 33]. *Botryosphaeria dothidea* chrysovirus 1 (BdCV1) and *Botryosphaeria dothidea* RNA virus 1 (BdRV1) are associated with hypovirulence in the fungal host [21, 24, 32]. *Botryosphaeria dothidea* victorivirus 1 (BdV1) has no obvious effects on the growth of host [33].

Here, we report a dsRNA virus isolated from *B. dothidea* EW220 and have designated the virus as *Botryosphaeria dothidea* botybirnavirus 1 (BdBRV1). BdBRV1 has a similar genome structure and 99% identity with BmBRV1 in nucleotide sequences. BdBRV1 confers hypovirulence to the host *B. dothidea* and could be transmitted via asexual sporulation. These characteristics permit its use as a potential biological control agent for diseases caused by *B. dothidea*.

## Materials and Methods

### Fungal isolates and culture conditions

Six strains of *B. dothidea* were used in this study (Table 1). Strain EW220 was isolated from a wart-diseased stem tissue of pear (*Pyrus bretschneideri* cv. Suli) grown in

Hubei Province in China. Strain JNT1111, which is highly virulent to pear fruits and shoots [30], was isolated from Shanxi Province in China and used as control in assessing biological features in this study. The virus-free strain EW220-64 was a single-conidium isolate of strain EW220. Strains EW220-64-T1, EW220-64-T2, and EW220-64-T3 from EW220-64 were obtained from a horizontal transmission assay. The strains were cultured on potato dextrose agar (PDA) plates at 28°C in the dark. Mycelial agar discs (5 mm) were stored in sterile 25% glycerol solution at -80°C.

**Table 1** Origin of strains of *Botryosphaeria dothidea* used in this study.

Strain	Origin	Mycovirus	Source
EW220	<i>Pyrus pyrifolia</i> , Wuhan, China	BdBRV1-infected	This study
JNT1111	<i>P. bretschneideri</i> , Shanxi, China	BdBRV1-free	This study
EW220-64	A single-conidium isolate of EW220	BdBRV1-free	This study
EW220-64-T1	EW220-64 in a pairing culture of EW220-64 and EW220	BdBRV1-infected	This study
EW220-64-T2	EW220-64 in a pairing culture of EW220-64 and EW220	BdBRV1-infected	This study
EW220-64-T3	EW220-64 in a pairing culture of EW220-64 and EW220	BdBRV1-infected	This study

## Extraction and purification of dsRNA

The strains were cultured on cellophane membranes overlaid on the surfaces of PDA plates for five days at 28°C in the dark. The mycelia were harvested and ground to a fine powder in liquid nitrogen. DsRNAs were extracted using a patented method (no. ZL201310072994.3). The dsRNA samples were digested with DNase I (RNase-free) and S1 nuclease (TaKaRa, Dalian, China) to eliminate any contaminating DNA and ssRNA. The purified dsRNA samples were subjected to electrophoresis in a 1% (w/v) agarose gel and viewed on a UV trans-illuminator after staining with 0.1 µg/mL ethidium bromide. The separated dsRNA segments were excised from the gel and purified using a DNA gel extraction kit (Axygen Scientific, Inc., Wujiang, China). The purified dsRNAs were dissolved in diethylpyrocarbonate (DEPC)-treated water and kept at -80°C.

## cDNA synthesis and molecular cloning

The full-length sequences of the purified dsRNAs were obtained as previously described [24]. The resulting products were ligated into a pMD18-T vector (TaKaRa, Dalian, China) and transformed into competent cells of *Escherichia coli* DH5α. All of the positive clones with inserts of more than 500 bp in size were sequenced. Sequence gaps between clones were determined by RT-PCR using primers designed from the obtained

cDNA sequences. The ligase-mediated rapid amplification of cDNA ends (RLM-RACE) procedure was conducted to obtain the terminal sequence of each of the dsRNAs as previously described [34]. Sequencing was performed by Genscript Biotechnology Co., Ltd., Nanjing, China. At least three independent clones of each product were determined in both orientations.

## Sequence analysis, alignment, and phylogenetic analysis

The DNAMAN software package (DNAMAN version 6.0; Lynnon Biosoft, Montreal, Canada) was used to detect potential open reading frames (ORFs). Prediction of the stem-loop structures of the terminal sequences of the viral RNAs were conducted using the RNA folding program from the Mfold website, with the default parameters (<http://mfold.rna.albany.edu/?q=mfold/RNA-Folding-Form2.3>) [35]. CD-search website of the National Center for Biotechnology Information (NCBI) (<http://www.ncbi.nlm.nih.gov/>) and the motif scan website (<http://www.genome.jp/tools/motif/>) were used to identify the conserved domains of the full-length cDNA virus sequences. MAFFT software [36] was used for multiple nucleotide and amino acid sequence alignments, and the results were visualized on BoxShade website ([http://www.ch.embnet.org/software/BOX\\_form.html](http://www.ch.embnet.org/software/BOX_form.html)). Phylogenetic trees were constructed using the maximum likelihood method in Molecular Evolutionary Genetics Analysis (MEGA) software 7 [37]. Bootstrap values (relative) generated using 1,000 replicates. Reference sequences of viruses used for comparative analyses were obtained from NCBI (<http://www.ncbi.nlm.nih.gov/genomes>).

## Virion purification

The purification of viral particles was performed as previously described [24]. Strain EW220 was grown at 28°C for 10 days on sterile cellophane films placed on PDA. About 20 g mycelia were harvested and ground into fine powder in liquid nitrogen. The powder was transferred to a container with 120 mL of 0.1 M sodium phosphate extraction solution (pH 7). The suspension liquid was centrifuged at 10,000 g for 20 min. The supernatant transferred to another plastic tube and then centrifuged at 10,000 g for 20 min again to remove any remaining hyphal cell debris. The supernatant was centrifuged at 100,000 g at 4°C for 2 h. The obtained pellet was re-suspended in 0.4 mL of 0.1 M phosphate buffer (PB, pH 7.0). The supernatant containing the virus particles was then overlaid on a centrifuge tube containing sucrose gradient (10%-50%, wt/vol) and centrifuged at 70,000 g at 4°C for 3 h. Each fraction was individually collected, and total RNA were extracted using phenol-chloroform and chloroform-isoamyl alcohol. Viral

dsRNAs were detected by 1% agarose gel electrophoresis. The fractions containing viral dsRNAs were centrifuged at 100,000 g at 4°C for 2 h, and the precipitate was suspended in 100 µL of 0.05 M PB. Viral particles were stained with 2% (wt/vol) uranyl acetate and examined by transmission electron microscopy (Model Tecnai G2 20; Field Electron and Ion Co.). The virus particle suspension was loaded onto a 12% polyacrylamide gel amended with 1% (wt/vol) sodium dodecyl sulfate (SDS) and ran for 8 h at 20 V/cm and stained with Coomassie brilliant blue R-250 (Bio-Safe CBB; Bio-Rad, USA). The separated proteins in SDS-PAGE were used for polypeptide mass fingerprinting-mass spectrum (PMF-MS) analyses.

## Biological Testing

Using previously described procedures [30], the mycelial growth rate, colony morphology, and virulence of virus-infected (EW220, EW220-64-T1, EW220-64-T2 and EW220-64-T3) and virus-free (EW220-64 and JNT1111) strains of *B. dothidea* were assessed (Table 1). Briefly, mycelial growth rates of the strains were measured on fresh PDA plates at 28°C. Each of the strains was assessed using six replicates. To evaluate the virulence of strain EW220, one-year-old shoots on five-year-old pear (*P. pyrifolia* cv ‘Hohsui’) plants grown in a field were used. The strains EW220 and JNT1111 were tested for their pathogenicity on unwounded shoots by directly placing colonized agar plugs (5 mm in diameter) on the surface of lenticels (shoots disinfested with 75% ethanol). Symptom development was monitored, and disease incidence was recorded at 60 days post inoculation (dpi). To assess for virulence of all of the tested strains, actively growing mycelial plugs from each strain were inoculated onto four detached pear fruits (*P. bretschneideri* cv. ‘Huangguan’). A PDA plug without the fungi was used as the non-inoculated control. Inoculated fruits were maintained in a 28°C incubator for four days, and then the average lesion size was measured. The experiment was repeated twice. The biological properties were investigated by one-way ANOVA using the SAS 9.0 program, and differences with *P*-values < 0.05 were considered statistically significant.

## Results

### Biological characteristics of strain EW220 and the detection of dsRNA

Strain EW220, which was cultured on PDA plates at the 28°C in the dark, exhibited abnormal growth. The mycelia grew slowly with few aerial hyphae (Figure 1A). The

developing colonies covered the whole dish (90-mm diameter) at ten dpi. In contrast, the virus-free strain JNT1111 grew rapidly, and developed numerous hyphae. The colony of strain JNT1111 could cover the entire culture dish at three dpi. The growth rate of the strain EW220 was only 30% of that of the strain JNT1111 (Figure 1A). The annual branches of pear tree (*P. pyrifolia* cv ‘Hohsui’) inoculated by strain EW220 showed no symptoms at 60 dpi (Figure 1B). However, the JNT1111 strain induced typical warts and canker symptoms (Figure 1B), and disease incidence reached 80%. These findings suggest that strain EW220 was a weak virulent strain.

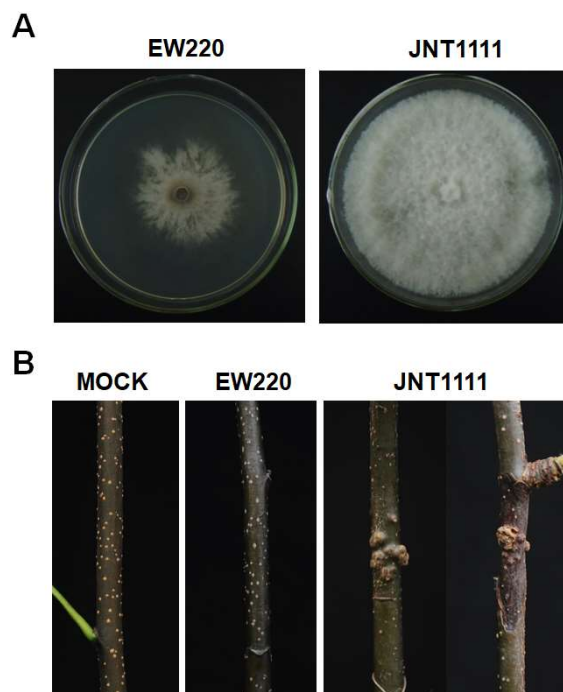


**Figure 1** Colony morphology and virulence of strain EW220 and strain JNT1111 on pear shoots (*Pyrus pyrifolia* cv ‘Hohsui’). (A) Colony morphology in PDA medium (28°C, 4 days). (B) Pear shoots unwound-inoculated with colonized plugs of tested strains and photographed at 60 days post inoculation.

DsRNA was extracted from strains EW220 and JNT1111. The results of 1.0% agarose gel electrophoresis showed that strain EW220 harbors dsRNA segments with sizes ranging from 7.0 kb to 7.5 kb. No dsRNAs were detected in the preparation from strain JNT1111 using the same treatment conditions (Figure 2A).

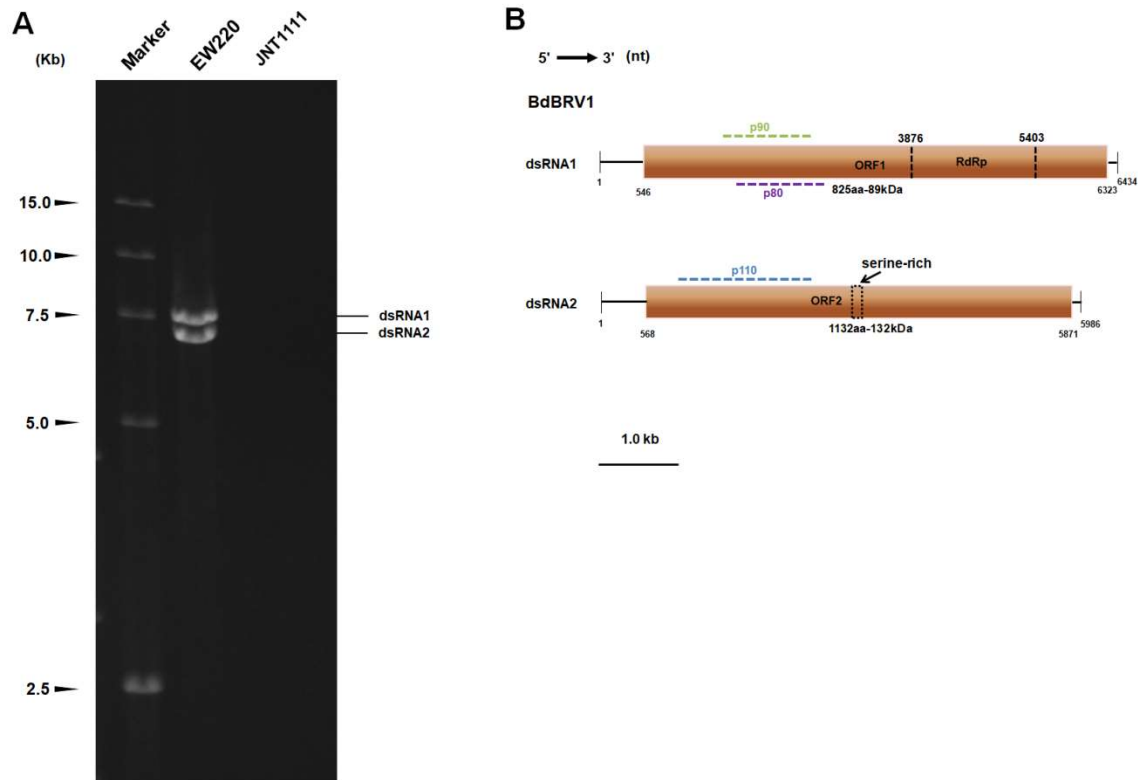


**Figure 2** Double-stranded RNAs extracted from strain EW220 and the genomic organization of *Botryosphaeria dothidea* botybirnavirus 1 (BdBRV1). (A) 1% agarose gel electrophoretic profiles of dsRNA preparations extracted from strains EW220 and JNT1111 after digestion with DNase I and S1 nuclease. (B) Genomic organization schematic diagrams of BdBRV1.

## Genetic analysis of dsRNAs

Based on the ds-cDNAs library, the 7.5-kb dsRNA generated 23 random fragments with lengths within the range of 800–2200 bp. BLAST analysis of its predicted amino acids indicates that these fragments encode a protein that was highly similar to the cap-pol fusion protein of BmBRV1 (sequence identities ranging from 99% to 100%). The 7-kb dsRNA generated a total of 18 random fragments with lengths ranging from 800 kb to 2,000 bp, BLAST analysis revealed that these sequences encoding amino acids that were most similarity to the hypothetical protein of BmBRV1 (sequences identities ranging from 99% to 100%). By combining the sequences obtained from RT-PCR and RLM-RACE, we obtained the cDNA sequences of the two segments of the dsRNAs. The full-length cDNAs of dsRNAs were 6,434, and 5,986 bp, respectively (Figure 2B). The corresponding sequences were deposited in GenBank under accession numbers



MH684534 and MH684535.

The cDNA length of dsRNA1 was 6,434 bp, with a GC content of 49.4%. BLASTn searches revealed that the dsRNA1 sequence shared high similarity (E-value = 0.0; 99% identity; 6,381/6,434 nt) with the dsRNA1 of the BmBRV1 (Supplementary Figure 1). A single large ORF from positions 546 nt to 6,323 nt was discovered, and this ORF encodes a tentative protein (P1) of 1,925 amino acid (aa) residues, with a mass of approximately 217 kDa. Motif scanning revealed that the P1 contained a conservative RdRp functional domain (RdRp\_4 Pfam02123) at its C terminal (Figure 2B). BLASTp analysis indicated that the protein was closely related to the cap-pol fusion protein of the members of genus *Botybirnavirus*, with 30% to 99% identities. In particular, P1 showed significant similarity to the cap-pol fusion protein of BmBRV1, which showed 99% identity (1,906/1,925 aa). The protein P1 was also most closely related to the cap-pol fusion protein of SsBRV1 with an identity of 82%. However, two amino acid fragments from 1 to 240 and from 901 to 1,080 of BdBRV1 exhibited low similarity with SsBRV1 (56% and 50% identities, respectively). Interestingly, an amino acid sequence (107 aa) encoded by the nucleotide sequence of dsRNA1 (from 3,462 to 3,785 nt) showed only 39% identity with SsBRV1 (Supplementary Figure 1). In addition, two bipartite nuclear localization signal profiles from amino acids 1,128 to 1,142 aa (KRAVYTIGTLLRKLK, *E* value = 2.1e-04) and from 1,417 to 1,431 (KRNSQLLEEKEERRR, *E* value=2.1e-04), a phosphatase tensin-type domain profile from 1,264 to 1,453 aa (*E* value=1.7e-02), a glutamine cyclotransferase from 1,333 to 1,346 aa (KLKSLGLKVDGHAN, *E* value = 0.0026), and an immunoreceptor tyrosine-based activation motif from 420 to 440 (TDLYNSIGDRAIAERYYDHVVT, *E* value=0.69) were also detected in the P1. The sequence of P1 was similar to the cap-pol fusion protein of SaBRV1, ABRV1, and BpRV1, sequence identities of 56%, 46%, and 30%, respectively.

The total length of the cDNA of dsRNA2 was 5,986 bp, with a GC content of 50.6%. BLASTn analysis shows that the sequence was most similar to BmBRV1 segment 2 (Supplementary Figure 2), showing 98% identity (*E* value=0.0; 5,886/5,986 nt). DsRNA2 also harbored a single ORF (ORF2, nt 568–5,671) on the genomic plus strand RNA. The protein (P2), which consisted of 1,767 amino acid residues and encoded by dsRNA2-ORF, was determined to have a molecular mass of 197 kDa (Figure 2B). A BLASTp search of P2 showed significant similarity to the hypothetical proteins of the members of genus *Botybirnavirus*, including BmBRV1 (99% identity; 1741/1767 aa), SsBRV1 (74% identity), ABRV1 (42% identity), SlaBRV1 (40% identity), SsBRV2 (28% identity), and BpRV1 (28% identity). Similarly, a nucleotide fragment of BdBRV1 from 3,630 to 4,326 nt had low similarity with SsBRV1 (58% identity, Supplementary Figure 2). The protein sequences (232 aa) encoded by this region were similar to a region of the hypothetical proteins, from 1,022 to 1,243 aa of SsBRV1, with 41% identity. In addition, an adenovirus GP19K from 18 to 41 aa (LLGCTSMFLFVEKTRGGVNLKKKMP, *E* value =



0.0025) and a serine-rich region profile from 1,039 to 1,084 aa (SNQSDADSDSDSGLARKSKPQQSLAKNLSSLKDSESESEASSSDDES,  $E$  value=1.3) were also found in P2 (Figure 2B).

The 5'-untranslated regions (UTR) of the coding strands of dsRNA1 and dsRNA2 were 545 bp and 567 bp in length, respectively. Similarly, the 5'-UTR of BmBRV1, BpRV1, ABRV1, SsBRV1, and SsBRV2 were 546/568 bp, 404 bp/405 bp, 544 bp/594 bp, 568 bp/577 bp, and 412 bp/411 bp in length, respectively [11–15]. The nucleotide sequences (about 498 bp) close to the 5'-terminus of dsRNA 1 and dsRNA 2 shared 97.8% sequence identity with each other (Figure 3A). Although a conserved terminal property was common in multipartite viruses, no long and strictly conserved sequences were detected in all known viruses, except for the members of family *Botybirnavirida* [11–15]. The corresponding 3'-UTRs were 111 bp and 115 bp in length, respectively, and the nucleotide sequences (about 71 bp) close to the 3'-terminus of dsRNA 1 and dsRNA 2 shared 84.3% sequence identity (Figure 3B). The secondary structures of the 5'- and 3'-UTRs of dsRNA 1 and dsRNA 2 were predicted to fold a stable stem-loop structure (Figure 3C). However, the stem-loop structure at the 3'-UTRs of dsRNA 2 was not detected.

Based on the genetic analysis of BdBRV1, we suggest that BdBRV1 and BmBRV1 were two strains of the same virus which infected different host fungi.

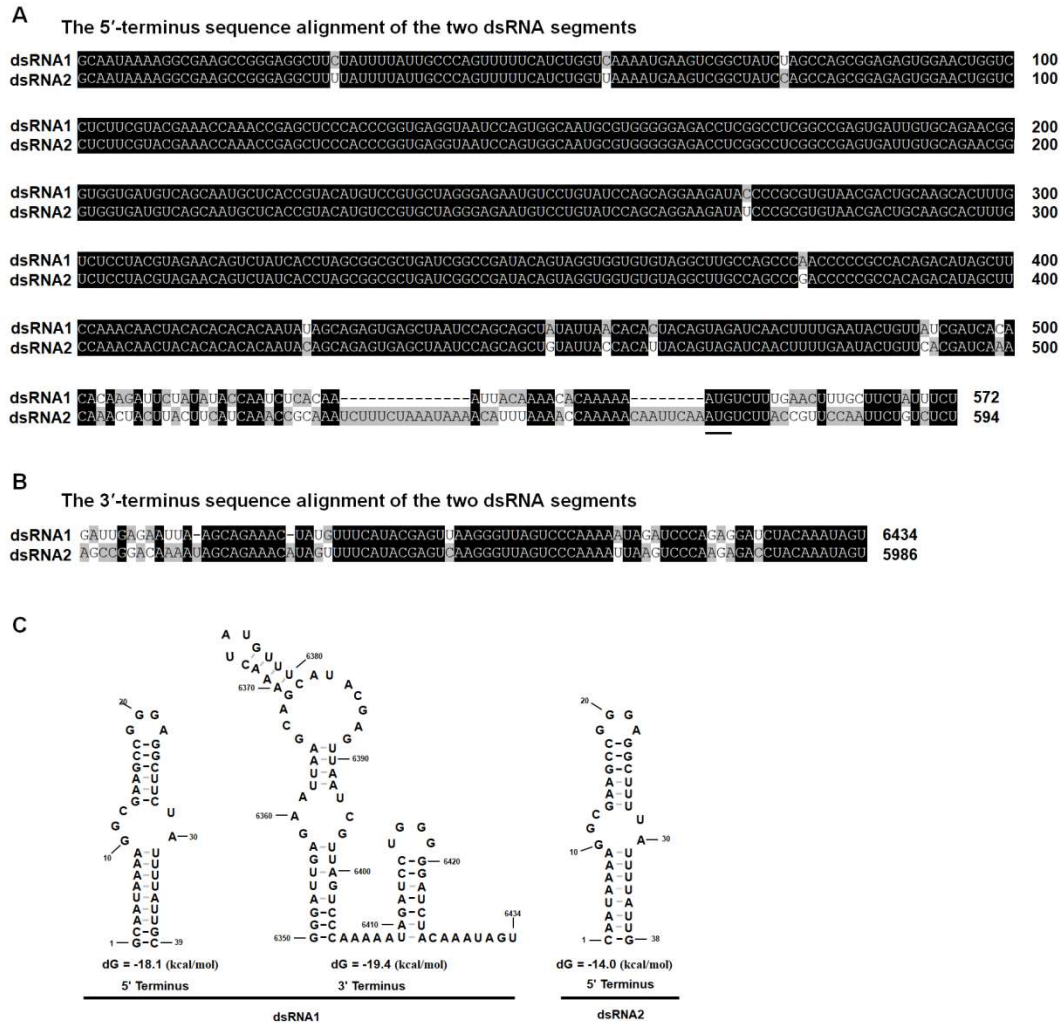


**Figure 3** Multiple-sequence alignments and predicted secondary structures for the terminal regions of the coding strand of dsRNA1 and dsRNA2. (A) Conserved sequence of 5'-UTRs and 3'-UTRs of dsRNA1 and dsRNA2; conserved sequences are shown in black. (B) Predicted secondary structures for the 5'- and 3'- terminus of the coding strands of dsRNA-1 and dsRNA-2 of BdBRV1.

## Phylogenetic analysis of the dsRNA virus

Multiple amino acid alignments of the predicted RdRp indicated the existence of the motifs I–VIII in BdBRV1 and other members of the family *Botybirnaviridae* (Figure 4A). A maximum-likelihood phylogenetic tree was constructed based on the amino acid sequences of RdRp encoded by members of families *Totiviridae*, *Partitiviridae*, *Chrysoviridae*, *Quadriviridae*, *Megabirnaviridae*, and some unassigned dsRNA viruses.

Phylogenetic reconstruction indicated that the members of the family *Botybirnaviridae* comprised two distinct clusters (Figure 4B). BdBRV1 was clustered together with BmBRV1, SsBRV1, ABRV1, and SIBRV1 to form a separate evolutionary clade from the other cluster, which contained BpRV1 (*Botybirnaviridae* mode) and SsBRV2 (Figure 4B).

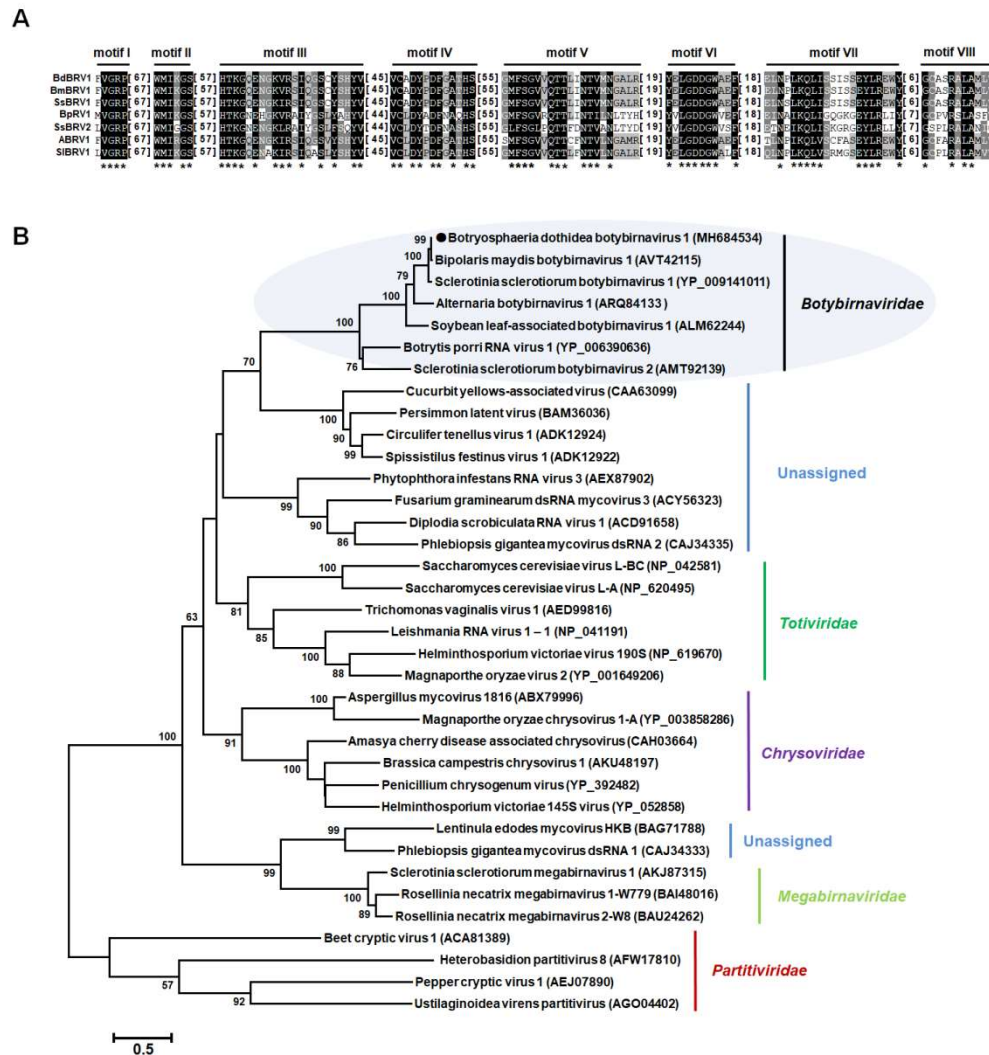


**Figure 4**

**Figure 4** Multiple alignments of the amino acid sequences of RNA-dependent RNA polymerase of BdBRV1 with other selected members in *Botybirnavirus* (A) and phylogenetic analysis of BdBRV1. The phylogenetic trees were constructed based on the best-fit model of protein evolution (LG + G + I + F). The gamma value was 2. Bootstrap values (relative) generated using 1,000 replicates are shown on the branches. Only  $\geq 50\%$  bootstrap values are presented, and branch lengths are proportional to the genetic distances. The red circle represents BdBRV1. Abbreviations: BdBRV1, Botryosphaeria dothidea botybirnavirus 1; BmBRV1, Bipolaris maydis botybirnavirus 1; SsBRV1, Sclerotinia sclerotiorum botybirnavirus 1; SsBRV2, Sclerotinia sclerotiorum

botybirnavirus 2; ABRV1, *Alternaria botybirnavirus* 1; SlBRV1, Soybean leaf-associated botybirnavirus 1; BpRV1, *Botrytis porri* RNA virus 1.

## Virus particles

Virus particles were purified from the mycelia of strain EW220 using sucrose gradient (10%–50% sucrose gradient fractions) centrifugation. Agarose gel electrophoresis of the nucleic acids extracted from the sucrose fractions showed that the dsRNA segments were mostly recovered from the 40% fraction. To examine the morphology of viral particles of BdBRV1, the fraction containing viral dsRNAs was centrifuged and re-suspended. The VLPs purified from strain EW220 were isometric and approximately 37 nm in diameter as observed under TEM (Figure 5A). Furthermore, the dsRNAs from the purified viral particles that were directly extracted from the mycelia of strain EW220 showed similar migration rates (Figure 5B). In addition, SDS-PAGE electrophoresis of the viral particles from the virus-infected strain EW220 revealed three major protein bands with approximate sizes of 110 kDa (p110), 90 kDa (p90), and 80 kDa (p80) (Figure 5C). However, compared to the other viruses of the family *Botybirnaviridae*, these differed in terms of size. The mechanism by which ORF1 and ORF2 specifically process or encode p110, p90, and p80 requires further investigation.

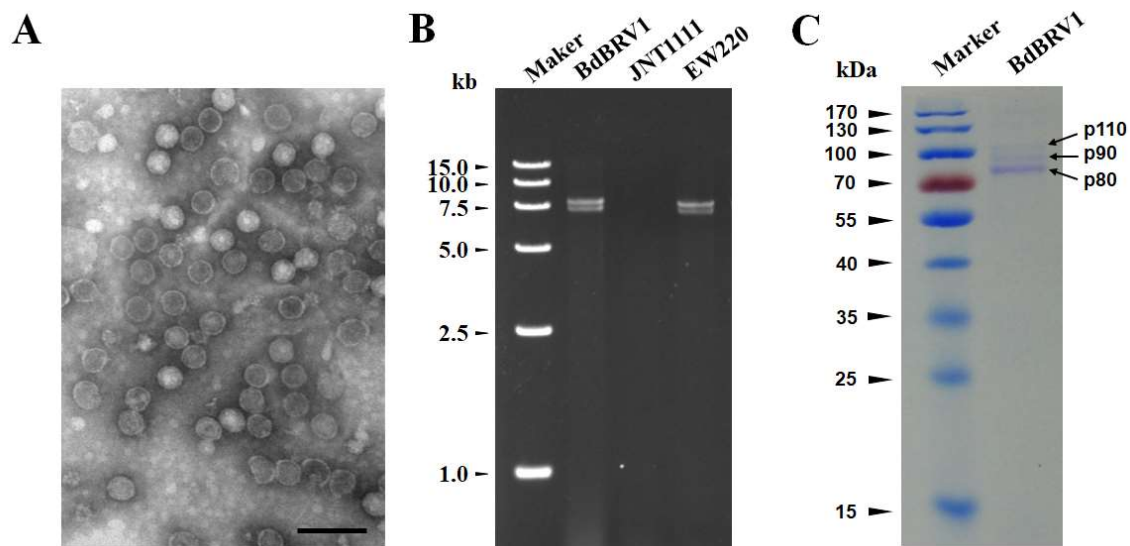


**Figure 5** Features of BdBRV1 viral particles (A) TEM images of BdBRV1 virus particles. (B) Agarose gel electrophoresis of the dsRNAs extracted from purified virus particles of BdBRV1 and the mycelia of strains EW220 (line EW220). (C) SDS-PAGE analysis of the purified virus particles shows the three distinct protein bands. The scale bar represents 50 nm.

## Analysis of virus structure proteins

To further analysis of virus structure proteins, the proteins of BdBBV1 virus particle preparations were loaded into SDS-PAGE and separated (Figure 5C). These were individually assessed and their corresponding genes determined using PMF-MS. A total of 13, 8, and 11 peptide fragments were discovered in p110, p90, and p80, respectively (Supplementary Tables S1–S3). The 110 kDa protein matched the partial sequence at amino acid 132–685 of P2 encoded by dsRNA2, accounting for 31.0% of the entire coverage (1767 amino acids). The 90 kDa protein matched the partial sequence at amino acid 323–865 of P1 encoded by dsRNA1, accounting for 28.0% of the entire coverage (1925 amino acids). The 11 peptides from p80 corresponded to an ORF1-encoded protein at the amino acid position of 383–865, accounting for 25.0% of the complete coverage (1925 amino acids). Based on the PMF-MS results, p110 was confirmed to correspond to the deduced 110-kDa proteins encoded by the ORF2 of dsRNA2, and p90 and p80 were encoded by the ORF1 of dsRNA1 (Figure 2B, Supplementary Tables S1–S3). Therefore, both ORF1 and 2 are involved in the structural proteins of BdBRV1 virus particles, and ORF1 actually encodes a cap-pol fusion protein. The structural proteins were derived from two ORFs encoded by dsRNA1 and dsRNA2 in the family *Botybirnaviridae* [10, 11, 13].

## Vertical and horizontal transmission of the dsRNA virus

Single-conidium strains were derived from strain EW220. Detection of dsRNAs revealed that strain EW220-64 was not infected by BdBRV1 (Figure 6), whereas others harbored dsRNA segments. This result revealed that BdBRV1 in strain EW220 was vertically transmitted to the conidium sub-strains. Furthermore, the dsRNA-free strains JNT1111 and EW220-64 were used as the recipients in the horizontal transmission assay. For each strain, three derivative sub-strains were obtained. The dsRNAs were recovered from the derivatives of the recipient strains. These results suggest that BdBRV1 from strain EW220 was horizontally transmitted to strains EW220-64T1, EW220-64T2, EW220-64T3 via hyphal contact (Figure 6). However, BdBRV1 from strain EW220 was not horizontally transmitted to the sub-strains from strain JNT1111 (data not shown). These results revealed that dsRNAs of BdBRV1 was successfully transmitted into isogenic fungal strain EW220-64, but not into strains with different of origins such as JNT1111, as earlier proposed for BpRV1 and SsBRV1 [11, 12].



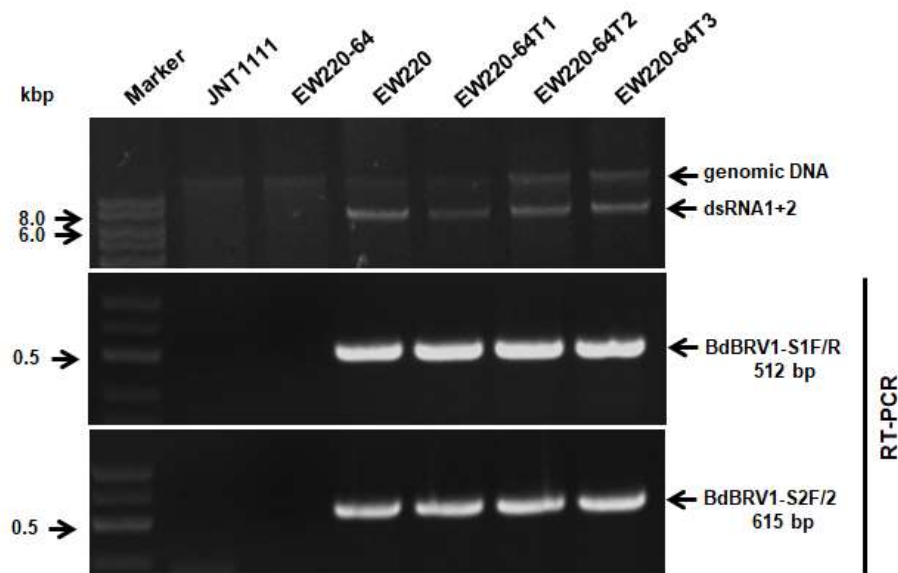


**Figure 6** Detection of BdBRV1 in different strains of *Botryosphaeria dothidea* by dsRNAs profiling and RT-PCR with specific primers. Strains EW220-64-T1, EW220-64-T2, and EW220-64-T2 were derived from EW220-64 in the pairing cultures of EW220/ EW220-64. The primers BdBRV1-S1F (5'-GCGCTGAGTGGATGATCAAAG-3') and BdBRV1-S1R (5'-CTCTTCGTCTGGCAAAAAGCC-3') were used for detecting BdBRV1-dsRNA1 segment, BdBRV1-S2F (5'-GCACTAAGAGAGACTTTCGAG-3') and BdBRV1-S2R (5'-CGGTAGGATC ATCCATAGTG-3') for detecting BdBRV1-dsRNA2 segment.

## Influence of BdBRV1 on the biological properties of *B. dothidea*

Biological assessment of the two BdBRV1-free and four BdBRV1-infected strains (Figure 6), including colony morphology, growth rate, and virulence, was performed. On PDA plates, the colonies of strains JNT1111 and EW220-64 exhibited radial growth and thick hyphae (Figure 7A). Compared to strains JNT1111 and EW220-64, the derivative strains (EW220-64T1, EW220-64T2, and EW220-64T3) grew slower on PDA at 28°C and formed abnormally whitish compact colonies (Figure 7A). The average growth rate of each tested strain varied from 14.6 mm/d to 37.5 mm/d. The average growth rate of the BdBRV1-infected strains EW220 (14.6 mm/day), EW220-64T1 (23.0 mm/day), EW220-64T2 (19.4 mm/day), and EW220-64T3 (20.7 mm/day) were significantly lower than that of EW220-64 (32.6 mm/day), which was an isogenic fungal strain from EW220 (Figure 7C). These results revealed that the BdBRV1 exerted greater influence on the growth rate of *B. dothidea*. The result of pathogenicity testing on the pear fruit revealed



that all of the tested strains caused rot lesions on the pear fruits. The average diameter of the lesions induced by strain EW220-64 (37.6 mm) was significantly larger than those induced by the isogenic fungal strains EW220 (12.3 mm), EW220-64T1 (24.3 mm), EW220-64T2 (12.9 mm) and EW220-64T3 (18.8 mm) (Figure 6C). Furthermore, the largest lesion was observed in JNT1111 (44.4 mm) (Figure 7B, C). Taken together, these findings indicate that BdBRV1 confers hypovirulence to the fungal host *B. dothidea*.

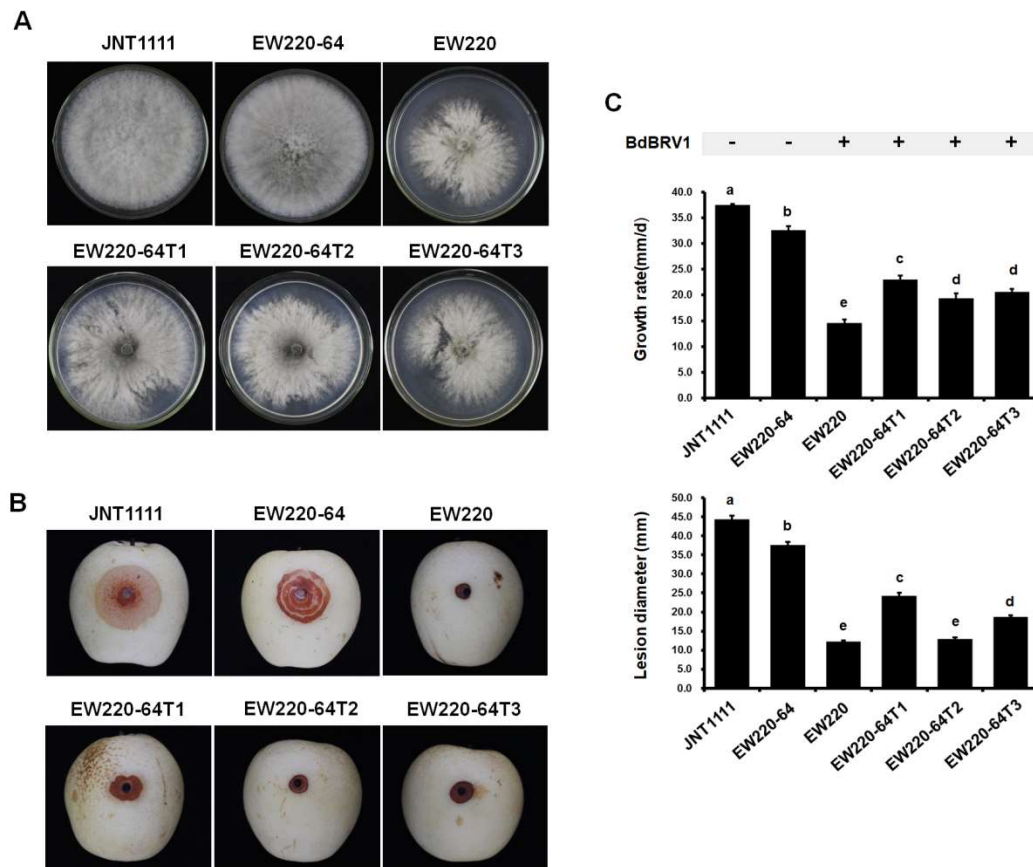


**Figure 7** Colony morphology and virulence of strain EW220, strain JNT1111 and derived sub-strains on pear fruit (*P. bretschneideri* cv. Huangguan). Strains EW220-64-T1, EW220-64-T2, and EW220-64-T2 were derived from EW220-64 in the pairing cultures of EW220/ EW220-64. (A) Colony morphology in PDA medium (28°C, 3 days). (B) Pear fruits wound-inoculated with colonized plugs of tested strains, and photographed at 4 days post inoculation. (C) Statistical analysis of the growth grate and the lesion size. The error bars indicate the standard deviations from different sample means. The letter indicates a significant difference at the  $P < 0.05$  level of confidence according to multiple range test.

## Discussion

This study represents the first report of a molecular and morphology characterization of a botybirnavirus, BdBBV1, which is the same sequence as BmBRV1. The largest dsRNA of BdBRV1 encodes a cap-pol fusion protein that contains part coat protein gene and a RNA-dependent RNA polymerase (RdRp) domain, and the second dsRNA encodes a hypothetical protein. BdBRV1 contains spherical virions that are 37 nm in diameter. Like BpRV1, SsBRV1, and ABRV1, BdBRV1 virus particles were constituted by different structural proteins. BdBRV1 influences the growth of *B. dothidea* and confers hypovirulence to the fungal host.

Currently, it was not report that the same mycovirus infects different fungi hosts. The host of BmBRV1 is *Bipolaris maydis* [16], which is the causal agent of corn southern leaf blight [38]. As a matter of fact, the *B. dothidea*, the host of BdBRV1, usual infected wood plants [24, 25]. Even though *B. maydis* and *B. dothidea* belong to the class Ascomycota, they have different hosts and biotopes. Our result might be the first funding in the different fungi infected by the same virus. In other hand, horizontal transmission experiments in this study indicated that BdBRV1 was successfully transmitted from strain EW220 into EW220-64, an isogenic fungus with strain EW220, but did not transmit into strains with different origins (strain JNT1111), as proposed before for BpRV1 [11]. These results reveal that the virus might not overcome the vegetative incompatibility in different strains. There might be one of the most important transmitted resources between different fungi hosts for realizing this event. One of the greatest example, Sclerotinia sclerotiorum hypovirulence associated DNA virus 1 (SsHADV-1) infects a mycophagous insect and utilizes it as a transmission vector [39]. Although this inference was consistent with the hypothesis that the might have spread horizontally between from *B. maydis* and *B. dothidea*. It did not rule out the possibility of the *B. dothidea* and *B. maydis* evolved from the same ancestor. Progenitor mycovirus infection and evolution antedates the radiation of *B. dothidea*/*B. maydis*.

Viruses of the family *Botybirnaviridae* consist of two dsRNAs. A satellite-RNA associated SsBRV1 has been identified [12], whereas no satellite RNA was detected in other botybirnaviruses-infected strains. Based on the results of phylogenetic reconstruction, the known viruses in family *Botybirnaviridae* comprise two different groups (see Figure 4B). BdBRV1 and BmBRV1 were more closely related to SsBRV1 than BpRV1 [15]. The nucleotide sequences of dsRNA1 and dsRNA2 of BdBRV1 were similar to the corresponding dsRNAs of SsBRV1, with 77% and 76% sequence identities, respectively [15]. Whereas, some regions of nucleotide sequences of BdBRV1 were showed lower identity (approximately 40%) with SsBRV1. The 5'-terminus of dsRNAs (about 498 bp) of BdBRV1 and BmBRV1 shared 87% sequence identity with the

5'-terminus of SsBRV1 (see Supplementary Figure 1, Supplementary Figure 2). It will be interesting to investigate which interrelation in BdBRV1, BmBRV1, and SsBRV1.

The genome organizations of BdBRV1 and BmBRV1 were consistent to BpRV1, SsBRV1, and SsBRV2, but differ from ABRV1 [11–16]. For example, BdBRV1-dsRNA1, SsBRV1-dsRNA1, and SsBRV1-dsRNA1 encode a cap-pol fusion protein containing an RdRp domain [11–13, 16]. However, in ABRV1, the cap-pol fusion protein is encoded by dsRNA2 [14]. The conserved terminal sequences of viral genomic RNA are generally involved in virus packaging [40, 41]. A long 5'-UTR and a relatively short 3'-UTR were highly conserved among the dsRNA segments of members of the family *Botybirnaviridae* [11–14, 16], for instance, approximately 500 bp at the 5'-UTRs and 100 bp at the 3'-UTRs of BdBRV1 (see Figure 3A). This kind of long and strictly conserved 5'- has not been observed in other known dsRNA viruses except botybirnaviruses [1, 11–15, 16]. In other hand, the first start codons (ATG) of ORF1 and ORF2 are located outside the strictly conserved region of 5' terminal of BdBRV1, BmBRV1 and SsBRV1 [12, 16], whereas those of BpRV1, SsBRV2, ABRV1 and are situated within the highly conserved region of 5'-UTR [11, 13, 14].

Members of family *Botybirnaviridae* consist of isometric viral particles of 35–38 nm in diameter [11–14]. Our result of the viral particles of BdBRV1 (37 nm in diameter) was in general agreement with previous morphometric studies [11–14]. The structural proteins might be derived from two ORFs encoded by dsRNA1 and dsRNA2 in the family *Botybirnaviridae* [11, 12, 14]. Three distinct protein bands of BdBRV1 were 110 kDa, 90 kDa, and 80 kDa. The protein p110 was encoded by the ORF2 of dsRNA2, and p90 and p80 were encoded by the ORF1 of dsRNA1 (see Supplementary Figure 3). In SsBRV1, the molecular weights of three structural proteins were 120 kDa (P120), 100 kDa (P100), and 80 kDa (P80) [12]. The P80 and P100 were encoded by ORF I (dsRNA1) and P120 encoded by the smaller fragment dsRNA2 (see Supplementary Figure 3) [12]. The three structural proteins of BpRV1 showed sizes of 85 kDa, 80 kDa, and 70 kDa [11]. PMF-MS analysis revealed that the 80- and 85-kDa structural proteins of BpRV1 are encoded by ORF I (dsRNA1), while the 70-kDa structural protein is encoded by ORF II (dsRNA2) (see Supplementary Figure 3) [11]. The three structural proteins of ABRV1 had sizes of 80 kDa, 70 kDa, and 60 kDa [14]. The isometric spherical particles of ABRV1 were putatively composed of three structural proteins encoded by ORF1 (p60) and ORF2 (p70 and p80) (see Supplementary Figure 3) [14]. Based on the data, the cap-pol fusion protein of botybirnaviruse contains two structural proteins and RdRp (see Supplementary Figure 3). The other hypothetical protein contains a structural protein (see Supplementary Figure 3). Differently, SsBRV2 comprised four structural protein components, with sizes of 100 kDa, 90 kDa, 70 kDa, and 60 kDa [13]. The structural proteins of other three botybirnaviruses were not described [15, 16]. It's worth digging into what the mechanism of the structural proteins exhibited different sizes in the family *Botybirnaviridae*. We also

found a serine-rich region profile in the BdBRV1-ORF2. In other botybirnaviruses, ABRV1-ORF2 contained a proline-rich region and SsBRV1-ORF2 contained a GHBP domain (animal growth hormone receptor binding domain) [12, 14]. However, those regions were not detected in SsBRV2, BmBRV1 and BpRV1 [11, 13, 15].

In the genus *Botybirnavirus*, BpRV1, SsBRV1, SsBRV2, ABRV1, and BmBRV1 infect filamentous fungi [11–14, 16], whereas SlaBRV1 was detected in a soybean phyllosphere via a metatranscriptomics technique [15]. Five mycoviruses in the family *Botybirnaviridae* have been identified to infect phytopathogenic fungi, but only two were involved in conferring hypovirulence to their host fungi [11, 12]. The results of the present study indicated that BdBRV1 is related to hypovirulence to *B. dothidea*. Similarly, BpRV1 and SsBRV2 could alter colony morphology and reduce the virulence of their host fungi [11, 13]. Interesting, *Sclerotinia sclerotiorum* strains infected SsBRV1 with a satellite-like RNA showed hypovirulence [12]. The satellite-like RNA (dsRNA 3) of SsBRV1 might play some roles in modulating the virulence of the virus [12]. Moreover, the ABRV1-infected fungal strains maintained active growth and a normal colony morphology but had attenuated virulence [14]. Our results confirm that BdBRV1 was closely associated with the hypovirulence of the phytopathogenic fungus.

In sum, we have characterized a bipartite dsRNA virus (BdBRV1) that infects *B. dothidea* strain EW220. Analysis of the genome organization and sequences indicate that BdBRV1 and BmBRV1 were two strains of the same virus. Phylogenetic reconstruction indicates that BdBRV1 and BmBRV1 were closely related to the recently proposed family *Botybirnaviridae*. The biological properties of virus-free and virus-infected strain EW220 revealed that BdBRV1 is the causal agent for hypovirulence. To the best of our knowledge, this is the first report of a botybirnavirus-infected fungus of *B. dothidea*.

**Author contributions:** Conceived and designed the experiments: Z.L., H.N., and W.G. Performed the experiments and analyzed the data: Z.L., Y.M., and Z.M., Wrote the paper: Z.L., and Z.M. Prepared tables and figures: Z.L., Z.M., and Y.M. Revised and approved the final version of the paper: Z.L., H.N., and W.G.

**Funding:** This work was financially supported through grants from The National Natural Science Foundation of China (31701837), the earmarked fund for Pear Modern Agro-Industry Technology Research System of the Chinese Ministry of Agriculture (CARS-28-15), the Fundamental Research Funds for the Central Universities (2662016PY107), the Yangtze Normal University Startup Foundation for Scientific Research (2017KYQD54), the Yangtze Normal University Scientific and Technological Foundation (2017XJQN10), and Plan for Supporting Development of Youth Scientific Research talent of Yangtze Normal University.

**Acknowledgments:** We give our special thanks to Professor Jiatao Xie from College of Plant Science and Technology, Huazhong Agricultural University, Wuhan, P.R. China, for giving suggestions during the study.

**Conflict of Interest Statement:** The authors declare no conflict of interest.

## References

1. Ghabrial, S.A.; Caston, J.R.; Jiang, D.; Nibert, M.L.; Suzuki, N. 50-plus years of fungal viruses. *Virology* **2015**, *479*, 356–368.
2. Ghabrial, S.A.; Suzuki, N. Viruses of Plant Pathogenic Fungi. *Annu. Rev. Phytopathol.* **2009**, *47*, 353–384.
3. Pearson, M.N.; Beever, R.E.; Boine, B.; Arthur, K. Mycoviruses of filamentous fungi and their relevance to plant pathology. *Mol. Plant Pathol.* **2009**, *10*, 115–128.
4. Xie, J.T.; Jiang, D.H. New insights into mycoviruses and exploration for the biological control of crop fungal diseases. *Annu. Rev. Phytopathol.* **2014**, *52*, 45–68.
5. Donaire, L.; Pagán, I.; Ayllón, M.A. Characterization of *Botrytis cinerea* negative-stranded RNA virus 1, a new mycovirus related to plant viruses, and a reconstruction of host pattern evolution in negative-sense ssRNA viruses. *Virology* **2016**, *499*, 212–218.
6. Liu, L.J.; Xie, J.T.; Cheng, J.S.; Fu, Y.P.; Li, G.Q.; Yi, X.H.; Jiang, D.H. Fungal negative-stranded RNA virus that is related to bornaviruses and nyaviruses. *Proc. Natl. Acad. Sci. USA* **2014**, *111*, 12205–12210.
7. Marzano, S.Y.L.; Nelson, B.D.; Ajayi-Oyetunde, O.; Bradley, C.A.; Hughes, T.J.; Hartman, G.L.; Eastburn, D.M.; Domier, L.L. Identification of diverse mycoviruses through metatranscriptomics characterization of the viromes of five major fungal plant pathogens. *J. Virol.* **2016**, *90*, 6846–6863.
8. Mu, F.; Xie, J.T.; Cheng, S.F.; You, M.P.; Barbetti, M.J.; Jia, J.C.; Wang, Q.Q.; Cheng, J.S.; Fu, Y.P.; Chen, T.; Jiang, D.H. Virome characterization of a collection of *Sclerotinia sclerotiorum* from Australia. *Front. Microbiol.* **2018**, *8*, 2540.
9. Wang, L.; He, H.; Wang, S.C.; Chen, X.G.; Qiu, D.W.; Kondo, H.; Guo L.H. Evidence for a novel negative-stranded RNA mycovirus isolated from the plant pathogenic fungus *Fusarium graminearum*. *Virology* **2018**, *518*, 232.
10. Yu, X.; Li, B.; Fu, Y.P.; Jiang, D.H.; Ghabrial, S.A.; Li, G.Q.; Peng, Y.L.; Xie, J.T.; Cheng, J.S.; Huang, J.B.; Yi, X.H. A geminivirus-related DNA mycovirus that confers hypovirulence to a plant pathogenic fungus. *Proc. Natl. Acad. Sci. USA* **2010**, *107*, 8387–8392.
11. Wu, M.D.; Jin, F.Y.; Zhang, J.; Yang, L.; Jiang, D.H.; Li, G.Q. Characterization of a novel bipartite double-stranded RNA mycovirus conferring hypovirulence in the phytopathogenic fungus *Botrytis porri*. *J. Virol.* **2012**, *86*, 6605–6619.
12. Liu, L.J.; Wang, Q.Q.; Cheng, J.S.; Fu, Y.P.; Jiang, D.H.; Xie, J.T. Molecular characterization of a bipartite double-stranded RNA virus and its satellite-like RNA co-infecting the phytopathogenic fungus *Sclerotinia sclerotiorum*. *Front. Microbiol.*



- 2015**, *6*, 406.
13. Ran, H.C.; Liu, L.J.; Li, B.; Cheng, J.S.; Fu, Y.P.; Jiang, D.H.; Xie J.T. Co-infection of a hypovirulent isolate of *Sclerotinia sclerotiorum* with a new botybirnavirus and a strain of a mitovirus. *Viol. J.* **2016**, *13*, 92.
  14. Xiang, J.; Fu, M.; Hong, N.; Zhai, L.F.; Xiao, F.; Wang, G.P. Characterization of a novel botybirnavirus isolated from a phytopathogenic *Alternaria* fungus. *Arch. Virol.* **2017**, *162*, 3907.
  15. Marzano, S.Y.L.; Domier, L.L. Novel mycoviruses discovered from metatranscriptomics survey of soybean phyllosphere phytobiomes. *Virus Res.* **2016**, *213*:332–342.
  16. Wang, H.R.; Li, C.; Cai, L.; Fang, S.G.; Zheng, L.M.; Yan, F.; Zhang, S.B.; Liu, Y. The complete genomic sequence of a novel botybirnavirus isolated from a phytopathogenic *Bipolaris maydis*. *Virus Genes* **2018**, *54*, 733–736.
  17. Tran, T.T.; Li, H.; Nguyen, D.Q.; Jones, M.G.K.; Wylie, S.J. Co-infection with three mycoviruses stimulates growth of a *Monilinia fructicola* isolate on nutrient medium, but does not induce hypervirulence in a natural host. *Viruses* **2019**, *11*, 89.
  18. Anagnostakis, S.L. Biological control of chestnut blight. *Science* **1982**, *215*, 466–471.
  19. MacDonald, W.L.; Fulbdght, D.W. Biological control of chestnut blight: use and limitations of transmissible hypovirulence. *Plant Dis.* **1991**, *75*, 656–661.
  20. Kamaruzzaman, M.; He, G.Y.; Wu, M.D.; Zhang, J.; Yang, L.; Chen, W.D.; Li, G.Q. A novel partitivirus in the hypovirulent isolate QT5-19 of the plant pathogenic fungus *Botrytis cinerea*. *Viruses* **2019**, *11*, 24.
  21. Wang, L.P.; Jiang, J.J.; Wang, Y.F.; Hong, N.; Zhang, F.P.; Xu, W.X.; Wang, G.P. Hypovirulence of the phytopathogenic fungus *Botryosphaeria dothidea*: association with a coinfecting chrysovirus and a partitivirus. *J. Virol.* **2014**, *88*, 7517–7527.
  22. Xiao, X.Q.; Cheng, J.S.; Tang, J.H.; Fu, Y.P.; Jiang, D.H.; Baker, T.S.; Ghabrial, S.A.; Xie, J.T. A novel partitivirus that confers hypovirulence on plant pathogenic fungi. *J. Virol.* **2014**, *88*, 10120–10133.
  23. Yu, X.; Li, B.; Fu, Y.P.; Xie, J.T.; Cheng, J.S.; Ghabrial, S.A.; Li, G.Q.; Yi, X.H.; Jiang, D.H. Extracellular transmission of a DNA mycovirus and its use as a natural fungicide. *Proc. Natl. Acad. Sci. USA* **2013**, *110*, 1452–1457.
  24. Zhai, L.F.; Xiang, J.; Zhang, M.X.; Fu, M.; Yang, Z.K.; Hong, N.; Wang, G.P. Characterization of a novel double-stranded RNA mycovirus conferring hypovirulence from the phytopathogenic fungus *Botryosphaeria dothidea*. *Virology* **2016**, *493*, 75–85.
  25. Zhai, L.F.; Zhang, M.X.; Hong, N.; Xiao, F.; Fu, M.; Xiang, J.; Wang, G.P. Identification and characterization of a novel hepta-segmented dsRNA virus from the phytopathogenic fungus *Colletotrichum fructicola*. *Front. Microbiol.* **2018**, *9*,

754.

26. Dissanayake, A.J.; Phillips, A.J.L.; Li, X.; Hyde, K.D. Botryosphaeriaceae: Current status of genera and species. *Mycosphere* **2016**, *7*, 1001–1073.
27. Marsberg, A.; Kemler, M.; Jami, F.; Nagel, J.H.; Postma-Smidt, A.; Naidoo, S.; Wingfield, M.J.; Crous, P.W.; Spatafora, J.W.; Hesse, C.N.; Robbertse, B.; Slippers, B. *Botryosphaeria dothidea*: a latent pathogen of global importance to woody plant health. *Mol. Plant Pathol.* **2017**, *18*, 477–488.
28. Tang, W.; Ding, Z.; Zhou, Z.Q.; Wang, Y.Z.; Guo, L.Y. Phylogenetic and pathogenic analyses show that the causal agent of apple ring rot in China is *Botryosphaeria dothidea*. *Plant Dis.* **2012**, *96*, 486–496.
29. Xu, C.; Wang, C.S.; Ju, L.L.; Zhang, R.; Biggs, A.R.; Tanaka, E.; Li, B.Z.; Sun, G.Y. Multiple locus genealogies and phenotypic characters reappraise the causal agents of apple ring rot in China. *Fungal Divers.* **2015**, *71*, 215–231.
30. Zhai, L.F.; Zhang, M.X.; Lv, G.; Chen, X.R.; Jia, N.N.; Hong, N.; Wang, G.P., Biological and molecular characterization of four *Botryosphaeria* species isolated from pear plants showing stem wart and stem canker in China. *Plant Dis.* **2014**, *98*, 716–726.
31. Yan, J.Y.; Xie, Y.; Zhang, W.; Wang, Y.; Liu, J.K.; Hyde, K.D.; Seem, R.C.; Zhang, G.Z.; Wang, Z.Y.; Yao, S.W.; Bai, X.J.; Dissanayake, A.J.; Peng, Y.L.; Li, X.H. Species of Botryosphaeriaceae involved in grapevine dieback in China. *Fungal Divers.* **2013**, *61*, 221–236.
32. Ding, Z.; Zhou, T.; Guo, L.Y. Characterization of a novel strain of *Botryosphaeria dothidea* chrysovirus 1 from the apple white rot pathogen *Botryosphaeria dothidea*. *Arch. Virol.* **2017**, *162*, 1–6.
33. Zhai, L.F.; Hong, N.; Zhang, M.X.; Wang, G.P. Complete dsRNA sequence of a novel victorivirus isolated from the pear stem wart fungus *Botryosphaeria dothidea*. *Arch. Virol.* **2015**, *160*, 613–616.
34. Liu, H.Q.; Fu, Y.P.; Jiang, D.H.; Li, G.Q.; Xie, J.T.; Peng, Y.L.; Yi, X.H.; Ghabrial, S.A. A novel mycovirus that is related to the human pathogen *Hepatitis E virus* and rubi-like viruses. *J. Virol.* **2009**, *83*, 1981–1991.
35. Zuker, M. Mfold web server for nucleic acid folding and hybridization prediction. *Nucleic Acids Res.* **2003**, *31*, 3406–3415.
36. Katoh, K.; Standley, D.M. MAFFT multiple sequence alignment software version 7: improvements in performance and usability. *Mol. Biol. Evol.* **2013**, *30*, 772–780.
37. Kumar, S.; Stecher, G.; Tamura, K. MEGA7: Molecular evolutionary genetics analysis version 7.0 for bigger datasets. *Mol. Biol. Evol.* **2016**, *33*:1870–1874.
38. Bruns, H.A. Southern corn leaf blight: a story worth retelling. *Agron. J.* **2017**, *109*, 1218–1224.
39. Liu S.; Xie J.T.; Cheng J.S.; Li B.; Chen T.; Fu Y.P.; Li G.Q.; Wang M.Q.; Jin H.N.;

- Hu W.H.; Jiang D.H. A Fungal DNA virus infects a mycophagous insect and utilizes it as a transmission vector. *Proc. Natl. Acad. Sci. USA* **2016**, *113*:128034–12808.
40. Anzola, J.V.; Xu, Z.K.; Asamizu, T.; Nuss, D.L. Segment-specific inverted repeats found adjacent to conserved terminal sequences in wound tumor virus genome and defective interfering RNAs. *Proc. Natl. Acad. Sci. USA* **1987**, *84*, 8301–8305.
  41. Wei, C.Z.; Saki, H.; Iwanami, T.; Matsumoto, N.; Ohtsu, Y. Molecular characterization of dsRNA segments 2 and 5 and electron microscopy of a novel reovirus from a hypovirulent isolate, W370, of the plant pathogen *Rosellinia*